SDSS'Rio 2010 STABILITY AND DUCTILITY OF STEEL STRUCTURES
E. Batista, P. Vellasco, L. de Lima (Eds.)
Rio de Janeiro, Brazil, September 8 - 10, 2010

FLANGE THICKNESS TRANSITIONS OF BRIDGE GIRDERS – BUCKLING BEHAVIOR IN GLOBAL BENDING

A. Lechner*, A. Taras* and R. Greiner*

* Institute for Steel Structures and Shell Structures, Graz University of Technology
Lessingstraße 25, A-8010 Graz, Austria
e-mails: lechner@TUGraz.at, taras@TUGraz.at, r.greiner@TUGraz.at

Keywords: Steel Bridges, Stability, Plate Girders, Local Buckling.

Abstract. *Flange thickness transitions constitute the most common constructional detail used to adapt the flexural resistance of bridge girders to variable bending moment distributions. The sudden change of stiffness distribution within the cross-section at these details causes additional local forces, stresses and deformations that cannot be properly taken into account by classical beam-theory calculations. Although these effects have been known in principle for some time, their correct inclusion in practical calculations has gained significance over the last years due to the use of thicker flange plates. The study presented in this paper focuses on the description of the realistic buckling behavior of bridge girder flanges at thickness transitions, whereby both linear and non-linear FEM calculations using shell elements are used and compared to the rather inaccurate predictions of the simple beam theory. One objective of this paper is also to give guidance to the designer concerned with the buckling strength of the girder flanges*.

1 INTRODUCTION

Flange thickness transitions and cover plates constitute two of the most common constructional details used to adapt the flexural resistance of bridge girders to variable bending moment distributions (Fig. 1). In the past, one or more additional cover plates have been added to flanges in riveted and welded constructions. Fig. 2 illustrates such constructional details used for welded girders, whereas flange thickness transitions can be provided by a variation in flange thickness only. The strengthening of the flange can be realized by flush upper edge, by centric arrangement or by flush lower edge, the latter allowing for an easier erection of laterally moved bridge girders.

Concerning the load carrying capacity of such flange thickness transitions, the buckling stability has to be verified with respect to the individual plate buckling slenderness of the two joined flanges. However eccentricity effects in connection with local imperfections, frequently caused by welding distorsion, need to be considered specifically. It has been observed that such local flange imperfections can be of considerable amount, see Fig. 2. Current codes for plate buckling, as Eurocode 3-1-5 [2], contain design provisions for plates with thickness transitions which recommend the use of transversal stiffeners for local restraint of these points.

In the present paper, the stability behavior will be investigated by means of linear buckling analyses (LBA) and geometrically materially nonlinear analyses including imperfections (GMNIA) using Abaqus [3], whereas in previous publications particularly the general stress state and the fatigue problem of flange thickness transitions have been addressed so far [5][6][7][8].

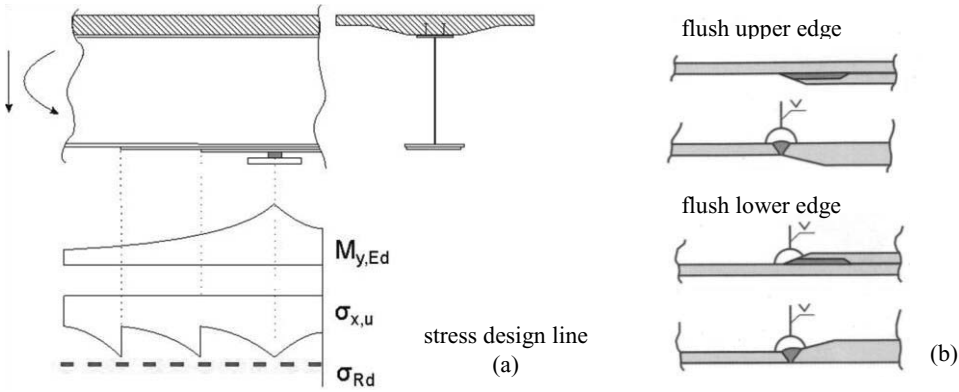

Figure 1: Overview of flange thickness transitions to adapt the flexural resistance of bridge girders in accordance with non-uniform bending moment distributions (a); constructional details with additional cover plates or with local variation in thickness of the flanges (b).

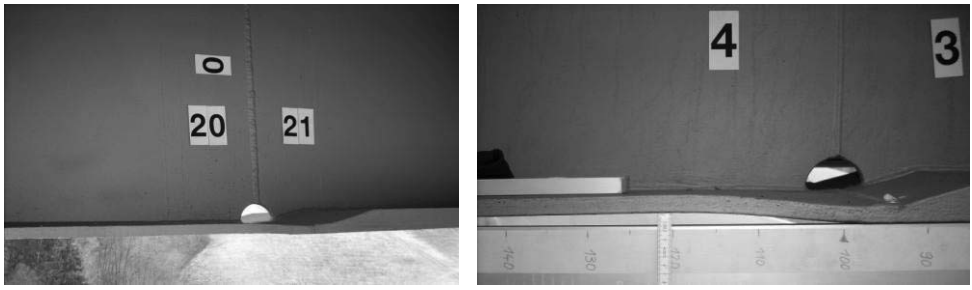

Figure 2: Geometrical imperfections in a large bridge girder, mainly caused by welding distorsion.

In Fig. 3 results of linear elastic analyses of a bridge girder with welded flange thickness transitions under uniform bending are shown. In the vicinity of the transition considerable additional shear in the web lower edge will be induced depending on the difference of axial force ΔN in the flanges due to the bending moment. The length of the decay of these forces is approximately the depth of the I-section. For the given case this would be 3500 mm. The results are plotted for three different flange configurations: flush upper edge (*fup*), *centric* and flush lower edge (*flo*). In case of *flo* the highest additional shear forces are induced, while *centric* causes the lowest effects.

A second effect should also be noted, i.e. the diagram of the axial flange forces which indicates a considerable increase of the flange force of the thinner flange when it approaches the point of the flange thickness transition. Since classical beam-theory disregards this effect totally, attention should be paid to it when considering the local flange buckling behavior in this region under compression.

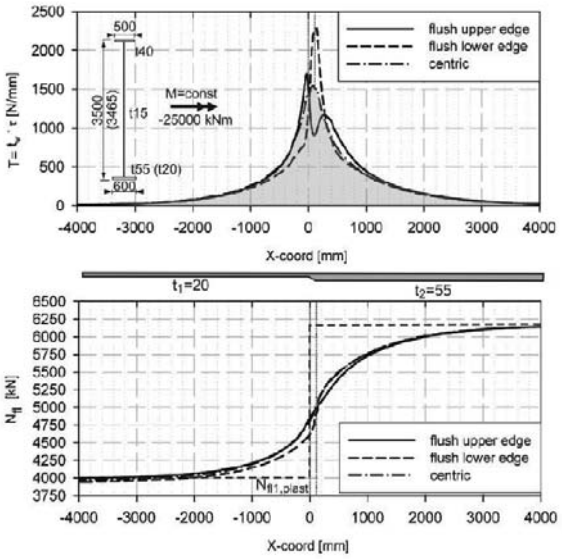

Figure 3: Elastic shear force distribution on web lower edge and axial force distribution in bottom flange.

2 ELASTIC CRITICAL BUCKLING BEHAVIOR

As a first step the local buckling behavior of the flange plate alone will be studied on basis of a three-sided supported plate with and without flange thickness transitions. The loading consists of a constant stress distribution σ_x across the width of the plate, acting in direction a. The numerical investigation has been carried out by using Abaqus [3] and the results have been compared to the analytical results from the classical Kirchhoff theory. (Approximately 8400 S4 – 4 node shell elements have been applied, shear effects were considered, 19 integration points were defined in thickness direction.)

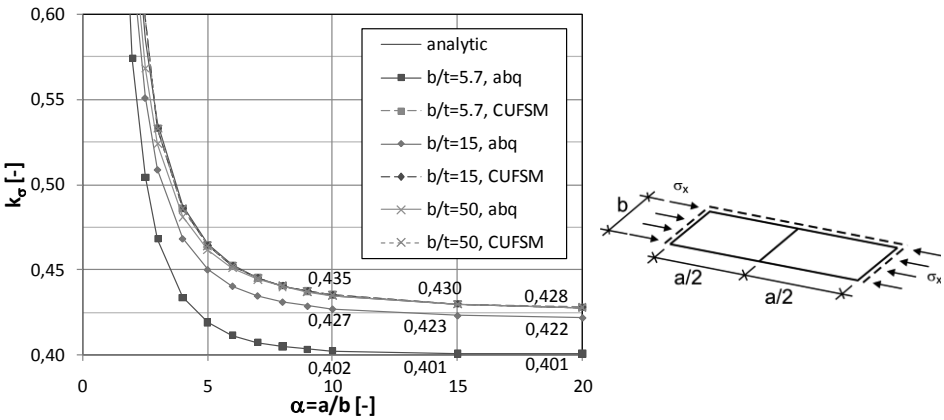

Figure 4: Plate buckling coefficients k_σ, comparison of FE-results with analytical solution and CUFSM.

Three different width-to-thickness ratios have been studied; the parameters are b/t = 5.7, 15 and 50, E = 210000 N/mm^2, ν=0.3. The results are shown by k_σ-α-curves in Fig. 4. In the calculations of the plates with constant thickness it was observed that the solution from Abaqus for thicker shells (b/t = 5.7) was app. 6% lower than the analytical result and the result from the Finite Strip Method CUFSM [4], which is due to the consideration of shear effects in the Abaqus analysis. In contrary the results for thin shells are fully coincident.

Then, the flange thickness transition of the plate was investigated. It was modeled by a definition of variable shell-thickness in the transition zone. The transition zone was placed in the half length of a.

It was found that the elastic plate buckling behavior is enhanced considerably depending on the thickness-ratio of the two adjacent flanges t_1/t_2. The k_σ-value can be doubled or even more for shorter plates (Fig. 5). A closer consideration of the results shows that for cases of $t_1/t_2 \geq 1.5$ local buckling is developed only in the thinner plate, since at the thickness transition the thicker plate provides support conditions for the thinner one.

The influence of different flange configurations on the buckling coefficients k_σ was also investigated. The results were nearly coincident for *fup*, *flo* and *centric* – only for short plates with a/b < 5 the buckling coefficients increase by app. 3 % for eccentric configuration compared to *centric*.

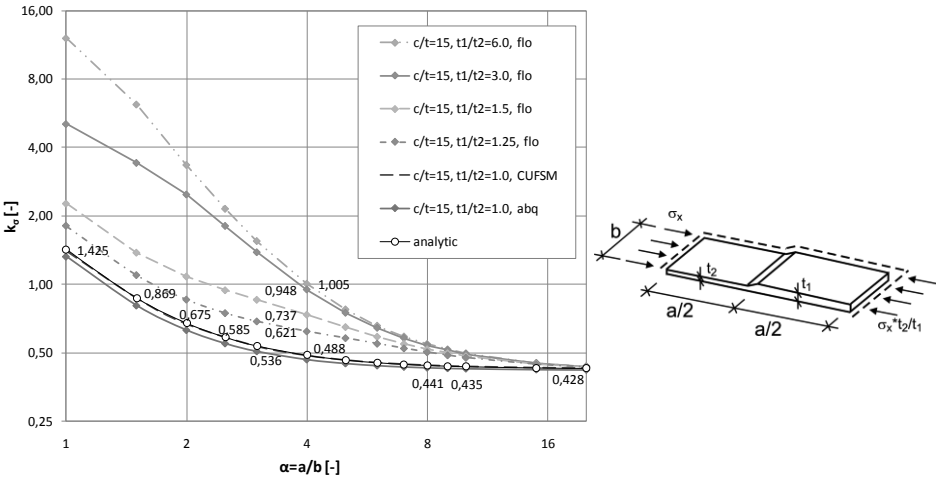

Figure 5: Plate buckling coefficients k_σ of plates with different flange thickness transitions t_1/t_2.

Moreover a supplemental buckling study on the I-sections of the girder with thickness transition in the compression flange was conducted. In this study only flange local buckling was allowed, while global buckling was excluded. Thereby the effects of the increase of the flange force of the thinner flange in the transition zone, which is shown in Fig. 3 above, have been investigated. The results were compared with the buckling results of the three-sided supported plate with thickness transition loaded by a constant axial force. It was found, that the recalculated buckling coefficients from the girder study were – with a variation of about +/- 8 % – close to those of the corresponding single plate with thickness transition.

3 NONLINEAR BUCKLING ANALYSES

3.1 Overview on numerical modeling

The focus of this investigation lies on the nonlinear analysis of girders with I-section with slender flanges in compression. Configurations with and without thickness transition (t_1/t_2) were considered. The nonlinear load carrying capacity of the girders was determined and compared with the results of the

classical beam theory, i.e. neglecting local effects at the transition point. Thereby, the results of I-sections with constant flange thickness serve as base values for the investigation of the nonlinear behavior of the sections with thickness transitions. In this publication only a ratio of t_1/t_2=3.0 is published (sect. 3.3), although a larger number of ratios t_1/t_2 has been investigated.

In the Finite-Element model, S4 – 4 node shell elements have been applied as for the flat plate before (sect. 2). The web and the upper flange were modeled by S4 elements with similar element size. The web-flange connections were modeled by pin-connectors, whereby all rotational degrees of freedom remained uncoupled. Pure local buckling was allowed in the compression flange (bottom flange), which means that in particular global stability effects and restraining effects of the web-flange conjunction have been disregarded. Imperfections were only applied to the compression flange by geometrical and structural imperfections. According to Eurocode 3-1-5 [2] the geometrical imperfections of the flange plates were modeled pursuant to the fabrication tolerances with an amplitude of 80 % of its tolerance limits. The residual stresses σ_R were modeled by the yield stress $\sigma_R=f_y$ in the welding zone and by $\sigma_R=-0.2*f_y$ in the remaining flange area, being in self-equilibrium and following a trapezoidal distribution shown in Fig. 6 in the diagram and by the FE-contour plot *increment 0*. The examples presented in this numerical study are based on a flange width of the bottom flange B_{bf} = 600 mm (= compression flange), which leads to a geometrical imperfection of e_0 = 4.8 mm, which is 80 % of $B_{bf}/100 = B_{bf}/125$. In the cases of flanges of constant thickness, the geometrical imperfection is assumed to follow its 1st buckling eigenmode. However in all cases of flanges with thickness transitions, the geometrical imperfections were modeled as local flange undulations according to [1] with an amplitude of e_0 = 4.8 mm, based on a gauge length equal to the flange width B_{bf}. In general, the nonlinear investigations presented herein are based on a length of the flange plate of a = 6000 mm. So far, girders with I-section were loaded in pure bending, leading to constant axial forces in the flange plates in the classical beam theory model. The load introduction at the end of the girders was realized by rigid I-sections, which were pin-connected to the adjacent shell elements of the flanges and the web.

In order to investigate the buckling behavior of these compression flanges of girders with I-section and to compare it with the corresponding buckling behavior of a three-sided supported plate with equal geometry and material, the numerical simulations have been carried out for single plates as well. Its results are included in the diagrams of the following sections 3.2 and 3.3.

3.2 Results of I-sections with constant flange thickness

In Fig. 6 the load displacement diagrams for the girders of I-sections with constant flange thickness are shown for three different assumptions of the local imperfection (i.e. e_0 = 3.0 mm resp. 4.8 mm with or without σ_R). On the abscissa the total vertical displacement U3 of the outmost node of the compression flange at midsection is plotted, which comprises the deformations caused by the global bending of the girder and those by the local buckling of the flange plate itself. On the vertical axis the non-dimensional load-carrying capacity resulting from Abaqus is shown, though divided by the section capacity of the effective cross-section according to [2]. For the given example, the compression flange was classified as Class 4 with a buckling reduction factor of ρ = 0.817, while in the web buckling was prohibited. The results show, that for the nonlinear analysis including geometrical and structural imperfections the section hardly can achieve the section capacity defined by [2]. In Figure 7 this is shown in the left diagram by the illustration of the forces in the compression flange. Regardless of the deformation state the EC 3 capacity of $N/N_{pl,bf}$ = 0.817 cannot be achieved, this means that only due to web plastification the load factor of 1.09 at increment 120 can be explained. The result of the FE-analysis of the flange plate alone (*plate*) achieves a similar result by $N_{GMNIA}/N_{pl,bf} \cong 0.70$.

On the contrary, Fig. 6 and Fig. 8 show for the analysis without residual stresses that the numerical simulation easily can achieve the EC3 design limit. A maximum load factor of 1.074 can be attained already at small deformations. The investigation of the normal force in the flange shows a result of $N_{GMNIA}/N_{pl,bf} \cong 0.9$, which is significantly beyond the design limit of ρ = 0.817 (Fig 8, left diagram).

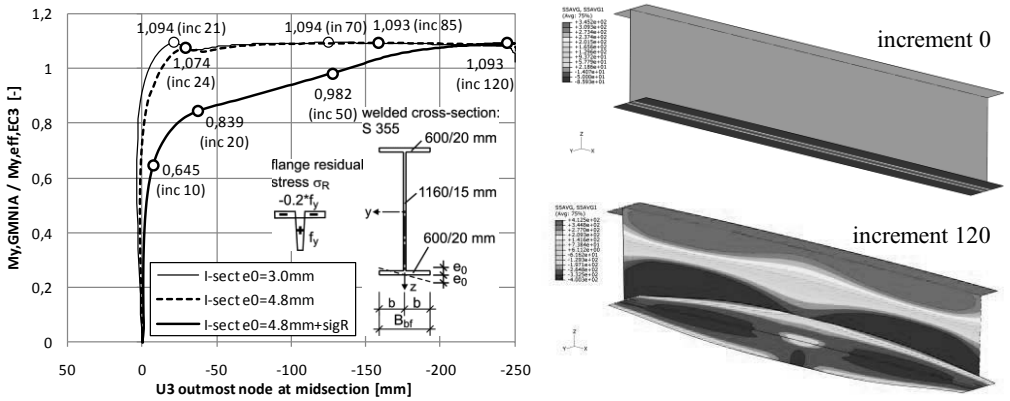

Figure 6: Load-displacement diagram for I-section with constant flange thickness and variation of buckling imperfections in bottom flange; GMNIA contour plots for increments 0 and 120, membrane stresses.

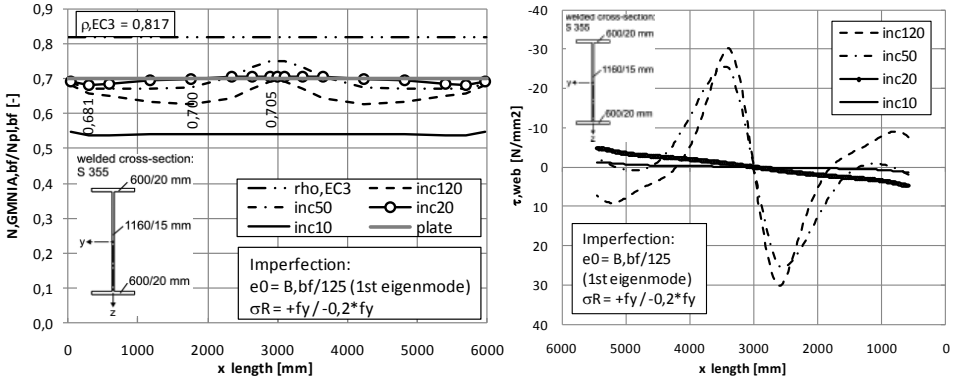

Figure 7: I-section with constant flange thickness, flange forces and shear stress at web bottom edge; with geometrical imperfections plus residual stresses.

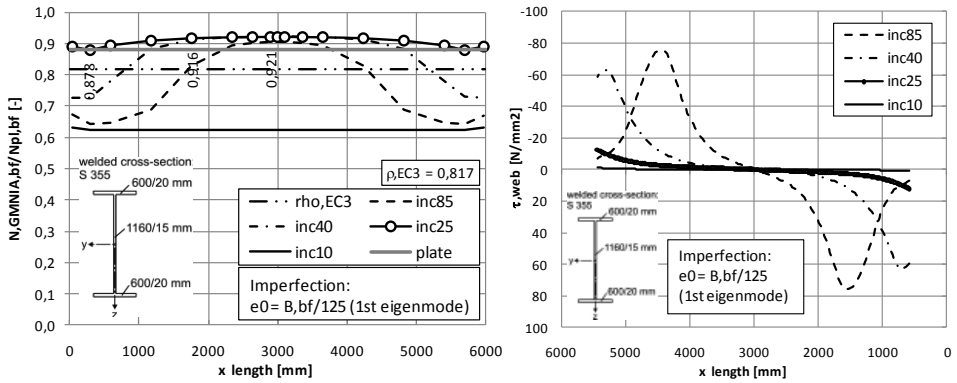

Figure 8: I-section with constant flange thickness, flange forces and shear stress at web bottom edge, with geometrical imperfections only.

In addition, shear stress distributions in the bottom web edge are plotted in Fig. 7 and Fig. 8. It was found that during local buckling of the flange plate a rather significant redistribution of flange axial force into the web occurs. This leads to these nonlinear axial force distributions along the axis of the girders.

3.3 Results of I-sections with flange thickness transition $t_1/t_2 = 3.0$

In Fig. 9 the load displacement diagrams of the girders with I-section with flange thickness transitions of t_1/t_2 = 60/20 mm = 3.0 are shown for four different configurations: a) geometrical imperfection $B_{bf}/125$ and residual stress σ_R, b) geometrical imperfection $B_{bf}/125$ only, c) imperfection type a) plus vertical web stiffener, d) imperfection type b) plus vertical web stiffener at the transition point.

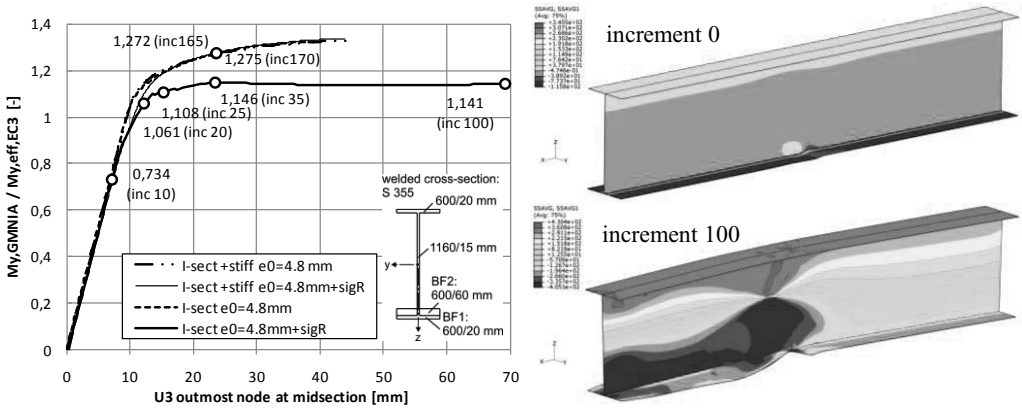

Figure 9: Load-displacement diagram for I-section, flange thickness transition t_1/t_2 = 3.00, variation of buckling imperfections on bottom flange; GMNIA contour plots for incr. 0 and 100, membrane stresses.

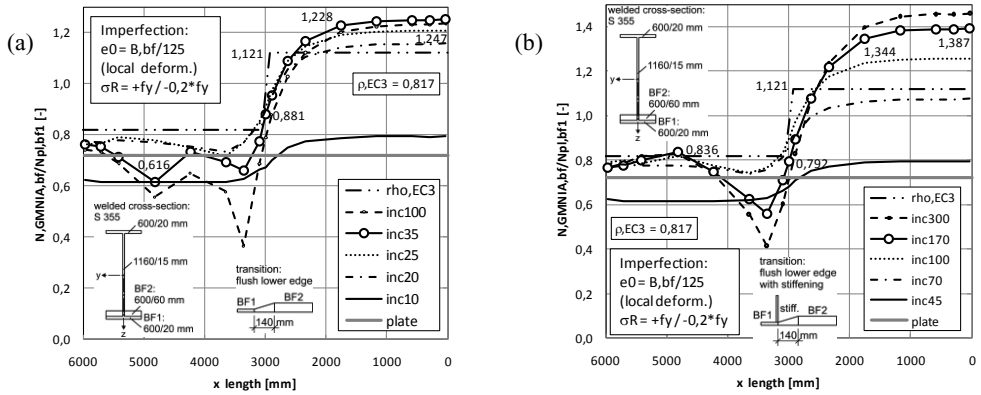

Figure 10: I-section with t_1/t_2 = 3.00, flange forces for configurations without (a) and with (b) vertical stiffener at the transition point.

By the comparison of these results with the results of the I-sections with constant flange thickness it turned out, that the nonlinear load-carrying capacity of the sections with thickness transitions is not as detrimental as expected. The GMNIA-analyses for all configurations with thickness transitions achieved more beneficial results compared to the corresponding girders with constant plate thickness. This can be seen in Fig. 9 in the left diagram by the nearly linear load-displacement path up to the nominal section capacity $M_{y,eff,EC3}$. In the GMNIA-contour plot *increment 100* it can be observed, although there is

considerable flange eccentricity at the transition point, that a significant restraining effect of the thicker flange on the thinner flange plate appears. The configuration a) without web stiffener leads to a factor of 1.14 by Abaqus, which is considerably beyond the EC 3-limit of 1.0. For the configuration c) with web stiffener at the transition point a maximum load factor of app. 1.34 has been achieved. The axial force distributions for the compression flange shown in Fig. 10 also illustrate this positive behavior.

For comparison, the *plate*-solution that is shown in Fig. 10 achieves a factor of $N_{GMNIA}/N_{pl,bf} = 0.72$, which is even larger than the result of 0.70 for constant flange thickness (sect. 3.2). It may be concluded, that the restraining effects caused by the thicker flange are more beneficial than the detrimental effects due to flange eccentricity. Considering beneficial restraining effects of the web, which have not been investigated in this publication, the results would lead to an even more conservative behavior.

11 CONCLUSION

Concerning flanges with thickness transitions, the rules according to EN 1993-1-5 [2] define vertical stiffeners in the thinner flange close to the transition point (Fig. 11 (b)). Since this requirement could not be confirmed by this numerical study, further investigations in combination with laboratory experiments should be performed. At present, one experimental test was carried out at the Laboratory for Structural Testing (LKI) at Graz University of Technology (Fig. 11(a)). By the evaluation of this test, the need for additional stiffeners according to EN 1993-1-5 could not be approved as well. More detailed results on this test will be presented in subsequent publications.

(a)

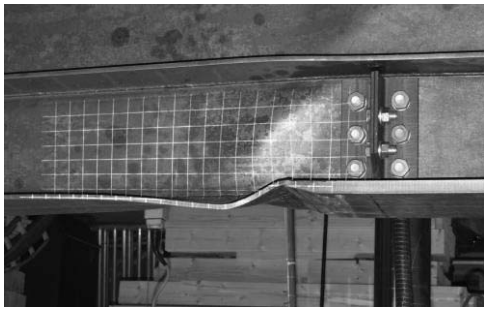

(b) EN 1993-1-5

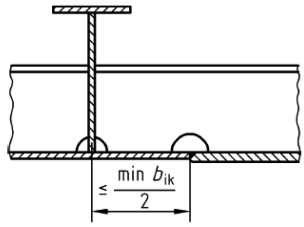

Figure 11: Laboratory test of I-section with flange thickness transition, LKI, Graz University of Technology (a); location of additional vertical stiffener according to EN 1993-1-5 (b).

REFERENCES

[1] EN 1090-2, *Execution of steel structures and aluminium structures – Part 2: Technical requirements for the execution of steel structures*, 2008.

[2] EN 1993-1-5, Eurocode *3, Design of Steel structures – Part 1.5. Plated structural elements*, 2007.

[3] ABAQUS v.6.7, Simulia, Providence, RI, USA, 2007.

[4] CUFSM v.3.12, Ben Schafer, JHU, Baltimore, USA, www.ce.jhu.edu/bschafer/cufsm, 2008.

[5] Stüssi, F., Dubas, P., *Grundlagen des Stahlbaues*, Springer Verlag, Heidelberg, Germany, 1971.

[6] Corfdir, P., Raoul, J., *Étude des contraintes au voisinage d'un raboutage de semelles d'épaisseurs différentes de poutres en I*, Construction Métallique, no 4-1990, 1990.

[7] Greiner, R., Taras, A., Unterweger, H., *Load-carrying behavior of flange-thickness transitions in welded steel girders*, Stahlbau 78, Heft 7, Ernst & Sohn Verlag, Germany, 2009.

[8] Lechner, A., Taras, A., *A numerical study of the fatigue proneness of flange thickness transitions in welded bridge girders*, Fatigue Design 2009, Cetim, Senlis, France, 2009.